PCCP

Accepted Manuscript

ROYAL SOCIETY OF CHEMISTRY

www.rsc.org/pccp

Synergistic Effects of Nonmetals Co-doping with Sulfur in Anatase TiO_2: A DFT+U Study

Qing-Lu Liu[1,3], Zong-Yan Zhao[2,*], Qing-Ju Liu[3,*]

[1] School of Physical Science and Technology, Yunnan University, Kunming 650091, People's Republic of China

[2] Faculty of Materials Science and Engineering, Key Laboratory of Advanced Materials of Yunnan Province, Kunming University of Science and Technology, Kunming 650093, People's Republic of China

[3] Yunnan Key Laboratory of Micro/Nano Materials & Technology, Research Institute of Engineering and Technology, Yunnan University, Kunming 650091, People's Republic of China

[*] Corresponding authors: zzy@kmust.edu.cn (Z. Zhao); qjliu@ynu.edu.cn (Q. Liu)

Abstract

Using DFT+U calculations, the crystal structure and electronic properties of nonmetals co-doing with sulfur in anatase TiO_2 are systematically investigated. The initial purpose of this work is to improve the photocatalytic performance of S mono-doped TiO_2, in which S occupies the lattice Ti site and acts as the recombination center. Among eight nonmetal impurities that occupy the interstitial site of TiO_6 octahedron, the synergistic effect of B, C, and O with S could achieve this purpose: suppressing the recombination of photogenerated electron-hole pairs by inducing local inner build-in electric field and eliminating the deep impurity energy bands of S mono-doped TiO_2. Furthermore, the photon absorption could be extended to visible-light region, owing to the overlapping of impurity energy bands with the top valence band or the bottom of conduction band. Thus, $Ti_{1-x}O_2S_xB_y$, $Ti_{1-x}O_2S_xC_y$ and $Ti_{1-x}O_2S_xO_y$ could be considered as the promising efficient photocatalysts. Furthermore, the underlying mechanism and tendency of these synergistic effects have been discussed, according to the relationship between photocatalytic performance and crystal or electronic structure.

1. Introduction

Since entering industrial era, environmental pollution and energy crisis are increasingly serious, and attract extensive concerns by the scientific researchers, industrial developers, or governments around the world. In a variety of solutions, photocatalysis technology are

extremely potential and promising, because they can utilize solar energy to product hydrogen by water splitting or to decompose the molecular pollutants. In this filed, titanium dioxide (TiO_2) acts the role of the typical representative and the prototype for the development of novel photocatalyst, owing to its various advantageous (such as low-cost, non-toxic, high-stability, etc.).[1-3] However, as a wide band gap semiconductor (~3.0 eV for rutile, ~3.2 eV for anatase), TiO_2 only presents photocatalytic activity under UV-light irradiation. What's more, its quantum efficiency is very low, due to the high recombination rate of photogenerated electron-hole pairs. In order to make the utmost of solar energy, there are several modification methods to enhance the photocatalytic activity of TiO_2 under visible-light irradiation, including: ions doping,[4, 5] noble metal loading,[6] semiconductor mixing, and dye sensitizing.[7, 8]

Among these modification methods, the ions doping is especially noteworthy, because its simplicity of synthesis and validity of modifying effects. Ion doping can not only increase carrier concentration and improve optical properties, but also form impurity energy band to capture photogenerated electrons or holes, resulting in suppress the recombination rate.[9, 10] However, the single ion doping is not always achieving these purposes. For example, metals doping suffer from some serious issues: thermal instability, recombination center of photognerated electron-hole pairs, and requirement of expensive ion-implantation facilities.[11, 12] What's more, if the impurity energy bands (or impurity induced energy bands, we did not distinguish these two concepts in this article) are located at the center of forbidden band, the probability of electrons and holes transition to them is equality, suggesting that they act as recombination center for photogenerated electron-hole pairs. Recently, researchers begin to attempt using ions co-doping to overcome these shortcomings of single ion doping, using the potential synergistic effects between different dopants. For instance, Li et al. reported that (C+H) co-doping produces significant band gap narrowing, which leads to higher visible-light photocatalytic efficiency than that of C-doped anatase TiO_2.[13] Some studies also suggest that the recombination rate of photogenerated electron-hole pairs could be further suppressed, if choosing appropriate ions co-doping into TiO_2 host.[14, 15]

For the co-doping modification, the basic design principle is producing impurity energy band that are overlapping with the top of valence band or the bottom of conduction band,

which could not only enhance the visible-light absorption but also guarantee photogenerated carries to transfer to reactive sites within their lifetime.[16-22] Although there are lots experimental studies for ions co-doping TiO_2 in recent years, there are still many difficulties and uncertainties: the synthesis methods and conditions are different, the evaluation criteria for the photocatalytic performance are not identical, and the process and influence factors of photocatalytic reaction are extremely complex. What's more, some reported experimental results are even contradictory, and the corresponding explanations are controversial. For example, In et al. reported that the visible light photoactivities of (B+N) co-doped TiO_2 are similar to B mono-doped TiO_2 for the degradation of methyl tertiary butyl ether, indicating the absence of synergy.[23] But Liu et al. considered the synergistic effects are responsible for the visible light absorption and the higher activity of (B+N) co-doped TiO_2.[24] Furthermore, due to random choose dopants to co-doping, there are no basis and rules to select the appropriate ions co-doping to improve the photocatalytic performance of TiO_2 under visible-light irradiation. Compared with experimental works, theoretical calculations can overcome the above shortcomings, and in-depth explore the interaction between the different dopants at the atomic-/electronic-scales. Gai et al.[25] develop a systematic understanding of the origin of electronic properties of 3d transition metals V and Cr, and 4d transition metals Nb and Mo substituting on the Ti site as the n-type dopants and N and C substituting on the O site as the p-type dopants. Their calculated results suggest (Mo+C) co-doped TiO_2 is an ideal candidate for hydrogen production by photocatalytic water splitting.

In our previous work, we found the impurity energy bands of S mono-doped anatase TiO_2, in which S atom occupies the lattice site of Ti, are located in the middle of the forbidden band. This type of impurity energy band maybe result in narrowing the band gap of TiO_2 to absorb visible-light, but acts as recombination center for the photogenerateed electron-hole pairs.[26] Furthermore, we have been designed efficient TiO_2-based photocatalyst by (N+V) co-doping,[27, 28] which have been confirmed by other research group's experiment,[29] and studied the effects on the water adsorption and decomposition.[30] Moreover, Harb et al.[2] proved that there is certain feasibility for S impurity to occupy the lattice site of Ti in anatase TiO_2 host. Therefore, it is necessary to further improve the photocatalytic performance of S-doped anatase TiO_2. On the other hand, there are a few theoretical calculations regarding

the origin of the S and nonmetal co-doping effects on anatase TiO_2, in which the compensation effect between anion ions and nonmetal ions maybe modify the disadvantage of S mono-doing. In order to find the appropriate ions to improve the photocatalytic performance of S mono-doped anatase TiO_2 by occupy the lattice site of Ti, and summary the basic co-doping effects of nonmetal ions, we chose nonmetal elements (B, C, N, O, F, P, S and Cl) as co-dopants, which are around S element in the Periodic Table, to interstitial dope into the vacancy of TiO_6 octahedron. By using GGA+U method, the calculated results can straight forward compare and summary. We will attempt to discuss the relationship between photocatalytic performance and electronic structures of ions co-doped TiO_2, and provide a possible explanation for experimental observations.

2. Computational methods

All calculations were performed in the framework of density functional theory within the generalized gradient approximation (GGA) using the PBE exchange correlation potential.[31-33] Utilizing the plane-wave total energy of ultra-soft pseudopotential method as implemented in CASTEP code to treat the ion-electron interaction.[34] The energy cutoff for plane wave basis set was 340 eV. In order to obtain accurate electronic structure, the method of GGA+U was adopted to overcome the well-known shortcoming of GGA.[35] The U value of 4.2 eV was applied to the Ti-d states and the O-p states, and other U value of 4.0 eV was applied to all the nonmetal (B, C, N, O, F, P, S and Cl)-p states. Using these values, the accurate band gaps could be obtained that could be compared with experimental measurements, as well as keeping the main features of electronic structure obtained by the standard DFT calculations. The Monkhorst-Pack scheme of K-points grid sampling was set as 2×2×2 for the irreducible Brillouin zone. A 120×120×120 mesh was used for fast Fourier transformation. The minimization algorithm was chosen the Broyden-Fletcher-Goldfarb-Shanno (BFGS) scheme. Its convergence criteria were set as follows: the force on the atoms were less than 0.01 eV/Å, the stress on the atoms were less than 0.02 GPa, the atomic displacement was less than 5×10^{-4} Å, and the energy change per atom was less than 5×10^{-6} eV. Based on the optimized crystal structure, the electronic structure and the optical properties were then calculated. Using above

mentioned computational method, we could obtain satisfactory as the reported results in recent studies.[36]

In the present work, a 3×3×1 supercell for anatase TiO_2 was used in constructing the doped models. For the S mono-doped TiO_2, one Ti atom is replaced by one S atom. For the nonmental mono-doped TiO_2, one nonmental atom (which will be labeled as "NM" in the following context) is inserted into the vacancy site of TiO_6 octahedron. For the S+NM co-doped TiO_2, one Ti atom is replaced by one S atom, as well as one NM atom is inserted into the near vacancy site of TiO_6 octahedron, while will be labeled as $Ti_{1-x}O_2S_xNM_y$ (NM = B, C, N, O, F, P, S and Cl). In the case of $Ti_{1-x}O_2S_xS_y$, in order to distinguish the two kinds of S atoms by different forms doping into TiO_2, we used S_s to denote the S atom that is replaced the Ti atom, and S_i to denote that the S atom that is inserted into the vacancy site. The denotation is also used in the case $Ti_{1-x}O_2S_xO_y$. Thus, the concentration of impurity is about 1.835% (atomic ratio), which is consistent with that of previous experiments.

3. Results and Discussion

3.1 Crystal Structure

To determine the most stable co-doping configuration, the total energy as function of distance between two impurity atoms is first discussed for every co-doping system. So, the lattice site of S replacing Ti atom is unchanged, and the NM atom is inserted into different TiO_6 octahedron. Then, the total energies of every co-doping configuration are compared, and the co-doping configuration with minimum total energy will be considered the most stable configuration. As example, Fig. 1(a) exhibits this relationship for $Ti_{1-x}O_2S_xN_y$. When N impurity is far away from the S impurity (distance larger than 4.5 Å), the total energy is almost identical, due to absence of the interaction between N and S impurities. When the distance in the range of 1.75~4.5 Å, the total energy is sharply decreasing that is arise from the attract interaction between N and S impurities, and finally reached the minimum at the distance of 1.75 Å. When the distance is smaller than 1.75 Å, the total energy is sharply increasing, due to the stronger repulsive interaction between N and S impurities. For the other seven co-doping system, the same tendency could be found, and the corresponding minimum

distances are listed in Table1 as S-NM bond length. These calculated results suggest that S and NM impurity will be gathered to together in anatase TiO_2 host by the strong atomic interaction. The most stable of co-doping system is schematic draw in Fig. 1(b).

To examine the relative difficulty for different impurity atom to incorporate into the host lattice sites, the impurity formation energies (E_f) are then discussed. The formation energy was calculated according to the formula that is defined by Van de walle et al. as following[37]:

$$E_f = E_{(doped)} - E_{(pure)} - \mu_S - \mu_{NM} + \mu_O + \mu_{Ti}$$

where $E_{(doped)}$ and $E_{(pure)}$ are the total energies with and without impurity. The chemical potential for Ti (μ_{Ti}) and O (μ_O) were calculated based on the formula $\mu_{TiO2} = \mu_{Ti} + 2\mu_O$. The μ_{NM} expresses the chemical potential for the nonmetal impurities. The calculated impurity formation energies of co-doping systems are tabulated in Table 1. In the practice, the ions doping is dependent on the growth condition (namely reducing or oxidizing condition). And the real experiments are usually carried out between these two extremes. So, the impurities formation energy of these eight co-doping systems and the S mono-doping system as function of oxygen potential difference are shown in Fig. 3. The smaller the E_f value means that the corresponding doping system could be easier carried out. In the present work, we found that the E_f value of these doping systems under the O-rich growth condition is negative and smaller than that of under the Ti-rich growth condition. This calculated result indicates that they are more stable under oxidizing conditions. It is worth notice that the E_f value of $Ti_{1-x}O_2S_xNM_y$ (NM = B, C, N, O, F, P, S and Cl) is increasing with the increase of impurity atomic number under when the nonmetal elements are in the same row of Periodic Table. The reason of this pheromone maybe ascribe the ion's radii is increasing with the increase of atomic number. Another important effect of co-doping is to design the synthesize route, namely the doping sequence.[28] For example, the E_f value of B mono-doping is very high (2.35 eV); while if B is doped into $Ti_{1-x}O_2S_x$ host, the E_f value could be decreased to -8.63 eV, which means S doping could improve the B incorporating into TiO_2 host.

Furthermore, the change of the bond length also present certain regularity: when the NM elements are in the same row of Periodic Table, the bond length of S-O and O-NM are increasing with the increase of atomic number; while the bond length of S-NM and Ti-NM are decreasing with the increase of atomic number. Corresponding, the change of bond length

leads to the volume of $Ti_{1-x}O_2S_xNM_y$ change. Owing to the radii of S ion is shorter than that of Ti ion, the volume of $Ti_{1-x}O_2S_x$ is smaller than that of TiO_2. However, because other NM impurities are inserted into the vacancy of TiO_6 octahedron, so the volumes of the co-doping systems are larger than that of pure TiO_2. And apart from the bond length, the change of the average net charge on the atoms also presents the certain regularity: when the impurity elements are in the same row of Periodic Table, the charge of O and S atoms become more and more lager with the increase of atomic number, which is opposite to that of NM atoms. Combined these calculated results, we found that the change tendency of these parameters has the same order with the change of electronegativity of NM elements: B<P<C<S< N<Cl<O<F (their electronegativities are 2.04, 2.19, 2.55, 2.58, 3.04, 3.16, 3.44 and 3.98, respectively).

As shown in Table 1, the changes of bond length, crystal volume, net charges on different atoms, which are caused by (S+NM) co-doping. And then, these changes will lead to a significant lattice deformation of octahedra, resulting in forming the build-in inner local electric field. This electric field could be reflected by the dipole moment of octahedral. In the pure TiO_2 system, the centers of positive charges and negative charges are coincided together, so the dipole moment of TiO_6 octahedron is zero. While, in the doping system, the center of positive charges is departing from the center of negative charges, so the corresponding dipole moment of octahedral are not equal to zero. Sato et al.[38] reported that the octahedral dipole moment is beneficial for the separation of photogenerated electronic-hole pairs within the local electric field, which can improve the photocatalytic activity of photocatalyst. Compared with S mono-doping, the dipole moment of octahedral in most co-doping system is obviously increased, implying that co-doing could enhance the photocatalytic performance of S mono-doping. In the present work, the dipole moment of $Ti_{1-x}O_2S_xS_y$ co-doping system is obviously larger than that of others, which suggests that it could be better suppress the recombination of photogenerated electron-hole pairs and may improve the photocatalytic performance of TiO_2.

3.2 Electronic structure

The calculated band structures of all doping systems are plotted and compared in Fig.3. Pure anataseTiO_2 is an indirect band gap semiconductor with a band gap of 3.210 eV, which

is very close to the experimental measurements (3.23 eV). The first doping effect is the slightly broadened band gap of $Ti_{1-x}O_2S_x$ system. In the cases of (S+NM) co-doping system, the band gap values of the $Ti_{1-x}O_2S_xNM_y$ (NM = B, C, N, P, and Cl) are smaller than that of pure TiO_2, while other three $Ti_{1-x}O_2S_xNM_y$ (NM = O, F, and S) have slightly broadened band gaps. Because these changes about band gap are very small, so this doping effect has limited influence to the light-absorption properties of TiO_2 host as shown Fig. S1 in Supplementary Information.

In the present work, the impurity energy states are the crucial factor that is determined the behavior of photogenerated electron-hole pairs. Compare to the pure TiO_2, S mono-doped TiO_2 exhibits the obvious feature: these is an impurity energy band located in the middle of band gap, which is contributed by the hybridization of S-3p states with its neighboring O-2p states and Ti-3d states, as shown in Fig. 3~4 and as mentioned in our previous work.[26] This type of impurity energy band is harmful for photocatalysis, and should be avoided, which is just the initial purpose of (S+NM) co-doping in the present work. In the cases of $Ti_{1-x}O_2S_xB_y$ and $Ti_{1-x}O_2S_xC_y$, there is no impurity energy bands located in the band gap, and the impurity energy bands are closed to the top of valence band (VB) (the minimum distance is 0.063 eV) in the case of $Ti_{1-x}O_2S_xO_y$. These calculated results suggest that B, C, and O co-doping with S could overcome the drawback of S mono-doping in the TiO_2 photocatalyst. However, in the rest cases of $Ti_{1-x}O_2S_xNM_y$ (NM = N, F, P, S, and Cl), there are more than two impurity energy bands in the band gap of TiO_2, especially in the case of $Ti_{1-x}O_2S_xF_y$. These impurity energy bands maybe improve the absorption of lower-energy photon, in which the lower-energy photons could excite the electron from VB to the impurity energy band and then to the conduction band (CB). In other words, these impurity energy bands maybe act as the role of intermediate step. However, they could act as recombination center for the photogenerated electron-hole pairs at the same time, owing to the near equal distance (namely equal transition possibility) with VB or CB as shown in Fig. 3. In Fig. 3~4, we assigned these figures as the position of NM in the Periodic Table, which could be better find the relationship between atomic features and the co-doping effects. In the same row, the positions of impurity energy bands are approximately shifting downward, as increasing the atomic number, except in the case of $Ti_{1-x}O_2S_xF_y$. This calculated result implies that different atomic

features of NM have different atomic interaction between two dopants and result in different co-doping effects. In the published literatures, the associated experimental works about sulfur co-doped TiO_2 are very limited. As examples, Sun et al. have been synthesized (S+C) co-doped TiO_2, and observed that the photocatalytic activity under visible-light irradiation;[39] Hamal et al. have demonstrated that TiO_2 co-doped with Ag, C and S can serve as a multifunctional generic biocide as well as a visible-light activated photocatalyst;[40] Zhang et al. considered that the high visible-light photocatalytic activity of the (S+N) co-doped TiO_2 may originate from the synergetic effect.[41] Compared with these experimental measurements, the calculated electronic structures of S+NM co-doped TiO_2 in the present work are consistent with them, and could explain the associated experimental phenomena.

To explore the chemical bonding information, the total and partial density of states (DOS) are provided in Fig. 4 and Fig. S2-S4 in Supplementary Information. The VB and CB of pure TiO_2 mainly consist of both the O-2p states and Ti-3d states, and the impurity energy bands are mainly contributed by the S-3p, O-2p and Ti-3d states, which are consistent with previous calculations.[42] For $Ti_{1-x}O_2S_xB_y$ and $Ti_{1-x}O_2S_xC_y$, there is no impurity energy bands located in the band gap, meanwhile, and we can find that the density of states of B-2p, C-2p and S_s-3p (in order to distinguish same atom in one doping system, we used the subscript "s" represent the substitutional impurity, and the subscript "i" represent the interstitial impurity in this article) are distributed in the whole range of VB and CB. For $Ti_{1-x}O_2S_xN_y$, $Ti_{1-x}O_2S_xF_y$, $Ti_{1-x}O_2S_xS_y$ and $Ti_{1-x}O_2S_xCl_y$, their impurity energy bands are mainly contributed by the S-3p, O-2p, Ti-3d and NM-np states. Different from the above co-doping systems, the impurity energy bands of $Ti_{1-x}O_2S_xO_y$ are mainly contributed by the O-2p, Ti-3d and O_i-2p states. The impurity energy bands of $Ti_{1-x}O_2S_xP_y$ is more special, which is contributed by the O-2p, Ti-3d and P-3p states and the other impurity energy level closer to the VB is contributed by the O-2p, Ti-3d and S-3p states. The NM-np states are somewhat delocalized, distributing in the almost whole range of VB and CB. Thus, the impurity energy bands are formed by O-2p states and Ti-3d states that are neighboring with impurity. The most outstanding peaks of DOS for the NM-np states are presented as following: the main B-2p states are distributed at the bottom of the VB; the main C-2p states are distributed for CB; the main N-2p states, P-3p states, S_i-3p states, and Cl-3p states are involved in the constitution of isolated impurity

energy bands, and meanwhile contributed to the consist of the bottom and top of VB; O_i-2p states and F-2p states are mainly involved in the constitution of the VB. Furthermore, we found that if the electronegativity of impurities are similar (for example, O and F, Cl and N, B and P), their np states have the similar position and contribution. Besides the contribution for the energy band formation, the co-doping of NM impurity could impact the electronic states of neighboring host atoms. And the most important influence is to form the impurity energy bands.

The Fig. 5 and Fig. 6 respectively provide the contour maps of electron density and electron density difference of the pure TiO_2 and all doping systems. Based on these maps, the further chemical bonding information and electron transfer could be obtained as following:

(1) For pure TiO_2, the chemical bonding between Ti and O mainly presents the feature of covalent bond. Due to the electronegativity of O (3.44) larger than the electronegativity of Ti (1.54), so O atom gets part of charges (-0.65 e, which is obtained from the analysis of Mulliken Atomic Populations as listed in Table 1), and Ti atom loses part of charges (1.68 e). And along with the d_{eq} bond direction, Ti atom loses more charges than that of along with d_{ap} bond direction.

(2) For $Ti_{1-x}O_2S_x$, due to the different atomic interaction, the bond length of S-O become longer, and the six bond lengths of S-O are no longer symmetrical. Among them, three of the S-O bond lengths longer than 2.3 Å, and the chemical bonding along these directions mainly presents the feature of ionic bond. The rest three S-O bond lengths are shorter than 1.6 Å, which mainly presents the feature of covalent bond. At the same time the adjacent Ti-O bond lengths are stretched to 2.27 Å, which presents the feature of ionic bond. Due to the electronegativity of S (2.58) smaller than the electronegativity of O, so O atom gets part of the charges (-0.68 e) and S atom loses part of charges (1.54 e).

(3) For $Ti_{1-x}O_2S_xB_y$, $Ti_{1-x}O_2S_xC_y$ and $Ti_{1-x}O_2S_xN_y$, due to the electronegativity of B (2.04), C (2.55) and N (3.04) is smaller than the electronegativity of O, which makes the local ionic bond turn into covalent bond (compared to $Ti_{1-x}O_2S_x$), but the Ti-O bond lengths in $Ti_{1-x}O_2S_xB_y$ and $Ti_{1-x}O_2S_xC_y$ are stretched longer (2.44 and 2.35 Å, respectively), which present the features of ionic bond. And for $Ti_{1-x}O_2S_xN_y$, the Ti-O bond lengths are shorted to 2.03 Å, which presents the feature of covalent bond.

(4) For $Ti_{1-x}O_2S_xO_y$, in which oxygen doping is belong to self-doping. Owing to the stronger atomic interaction between interstitial O impurity and substitutional S impurity, they form the SO_x-molecule-like aggregate. Thus, three S-O bond lengths and one Ti-O bond length are becoming longer, and the corresponding feature of ionic bond is becoming more prominent.

(5) For $Ti_{1-x}O_2S_xF_y$ and $Ti_{1-x}O_2S_xCl_y$, due to the electronegativity of F (3.98) is very strong and more electrons concentrate around F impurity, the feature of covalent bond of Ti-O bonds and S-O bonds that are surround F impurity are becoming less prominent. At the same time, F impurity plays the role of bridge to form S-O-Ti link. For Cl co-doping system, the similar phenomenon could be found. However, because the electronegativity of Cl (3.16) is relatively smaller than that of F, so the related phenomenon is not obvious.

(6) For $Ti_{1-x}O_2S_xP_y$, P impurity is inserted between two lattice oxygen atoms, and acts as the role of bridge to link them. So the PO_x-molecule-like aggregate is also formed, with obvious features of covalent bond. At the same time, covalent bands between S atom and P impurity or O atom are formed. In addition to the original Ti-O ionic bond (its bond length is elongated to 2.32 Å), another stretched Ti-O bond (2.15 Å) presents the features of ionic bond.

(7) For $Ti_{1-x}O_2S_xS_y$, the S_s and S_i show a very strong atomic interaction, and thus are forming the S_x-molecule-like aggregate. Meanwhile, the most obvious phenomenon is that the features of covalent bond are more prominent in the whole range of co-doping system.

4. Summary and Conclusions

The DFT+U method were adopted to analyze the synergistic effects of nonmetals co-doping with sulfur in anatase TiO_2 in the present work. The initial purpose of nonmetals co-doping in this present work is to improve the drawback of S mono-doping that was found in our previous work. It is shown that B, C and O (that occupies the interstitial site of TiO_6 octahedron) co-doping with S (that replaces Ti) are expected to facilitate improve the photocatalytic performance of anatase TiO_2. Based on the calculated results, some conclusions were summarized as following: (1) The electronegativity partially determines the

direction and the quantity of the electron transfer in the co-doping systems, and has certain relevance to the formation of impurity energy bands. However, it is not the only factor that decides where the impurity energy bands present in the band gap. (2) Whether the impurity energy bands present in the band gap mainly depend on the compensation effect between nonmetal impurities and sulfur impurity. When Ti is replaced by S, the charge balance is consequently broken. Thus, if the interstitial impurity could compensate this charge imbalance, as well as cause slight lattice distortion and form stable local microstructure, the related impurity energy bands could disappear in the band gap or overlapping with VB or CB. Thus, to design co-doping systems should consider the combination influence between electronegativity, valence state, the number of valence electrons, and the atomic interaction between impurities. In other words, the synergistic effects of co-doping are the comprehensive results. (3) For the $Ti_{1-x}O_2S_x$ photocatalyst, B and C co-doping or intended O self-doping are the effective ways to improve its photocatalytic performance, ascribing from the synergistic effects. Therefore, $Ti_{1-x}O_2S_xB_y$, $Ti_{1-x}O_2S_xC_y$ and $Ti_{1-x}O_2S_xO_y$ could be considered as the promising efficient photocatalyst. Based on the calculated results, some guidance could be provided for the future experimental works: the co-doping could be easier achieved through the step synthesis process; to select two dopants that have compensation effects and larger difference of electronegativity could be better meet the design requirement of efficient photocatalyst via ions co-doping; nonmetal ions with variable valence states could easier realize effective synergistic effects of co-doping for TiO_2 photocatalyst.

Acknowledgements

The authors would like to acknowledge financial support from the National Natural Science Foundation of China (Grant No. 51062017 and 51262030).

Reference

1. T. Ohno, M. Akiyoshi, T. Umebayashi, K. Asai, T. Mitsui and M. Matsumura, *Appl. Catal. A*, 2004, **265**, 115.
2. M. Harb, P. Sautet and P. Raybaud, *J. Phys. Chem. C*, 2013, **117**, 8892.
3. T. Umebayashi, T. Yamaki, H. Itoh and K. Asai, *Appl. Phys. Lett.*, 2002, **81**, 454.
4. T. Umebayashi, T. Yamaki, S. Yamamoto, A. Miyashita, S. Tanaka, T. Sumita and K. Asai, *J. Appl. Phys.*, 2003, **93**, 5156.

5. J. Liqiang, S. Xiaojun, X. Baifu, W. Baiqi, C. Weimin and F. Honggang, *J. Solid State Chem.*, 2004, **177**, 3375.
6. K. Hiehata, A. Sasahara and H. Onishi, *Nanotechnology*, 2007, **18**, 084007.
7. F. Chen, Z. Deng, X. Li, J. Zhang and J. Zhao, *Chem. Phys. Lett.*, 2005, **415**, 85.
8. B. O'regan and M. Grfitzeli, *Nature*, 1991, **353**, 737.
9. X. Chen and S. S. Mao, *Chem. Rev.*, 2007, **107**, 2891.
10. K. Singh, J. Nowotny and V. Thangadurai, *Chem. Soc. Rev.*, 2013, **42**, 1961.
11. H. Yamashita, M. Honda, M. Harada, Y. Ichihashi, M. Anpo, T. Hirao, N. Itoh and N. Iwamoto, *J. Phys. Chem. B*, 1998, **102**, 10707.
12. Y. Wang, H. Cheng, Y. Hao, J. Ma, W. Li and S. Cai, *Thin Solid Films*, 1999, **349**, 120.
13. N. Li, K. L. Yao, L. Li, Z. Y. Sun, G. Y. Gao and L. Zhu, *J. Appl. Phys.*, 2011, **110**, 073513.
14. S. G. Kumar and L. G. Devi, *J. Phys. Chem. A*, 2011, **115**, 13211.
15. J. Zhang, Y. Wu, M. Xing, S. A. K. Leghari and S. Sajjad, *Energy Environ. Sci.*, 2010, **3**, 715.
16. R. Asahi, T. Morikawa, T. Ohwaki, K. Aoki and Y. Taga, *Science*, 2001, **293**, 269.
17. W. Zhu, X. Qiu, V. Iancu, X.-Q. Chen, H. Pan, W. Wang, N. M. Dimitrijevic, T. Rajh, H. M. Meyer Iii, M. P. Paranthaman, G. M. Stocks, H. H. Weitering, B. Gu, G. Eres and Z. Zhang, *Phys. Rev. Lett.*, 2009, **103**, 226401.
18. Y. Gai, J. Li, S.-S. Li, J.-B. Xia and S.-H. Wei, *Phys. Rev. Lett.*, 2009, **102**, 036402.
19. N. Feng, Q. Wang, A. Zheng, Z. Zhang, J. Fan, S.-B. Liu, J.-P. Amoureux and F. Deng, *J. Am. Chem. Soc.*, 2013, **135**, 1607.
20. J. Schneider, M. Matsuoka, M. Takeuchi, J. Zhang, Y. Horiuchi, M. Anpo and D. W. Bahnemann, *Chem. Rev.*, 2014, **114**, 9919.
21. M. Khan, J. Xu, N. Chen, W. Cao, Asadullah, Z. Usman and D. F. Khan, *Res. Chem. Intermediat*, 2013, **39**, 1633.
22. F. Yang, H. Yang, B. Tian, J. Zhang and D. He, *Res. Chem. Intermediat*, 2013, **39**, 1685.
23. S. In, A. Orlov, R. Berg, F. Garcia, S. Pedrosa-Jimenez, M. S. Tikhov, D. S. Wright and R. M. Lambert, *J. Am. Chem. Soc.*, 2007, **129**, 13790.
24. G. Liu, Y. Zhao, C. Sun, F. Li, G. Q. Lu and H.-M. Cheng, *Angew. Chem. Int. Ed.*, 2008, **47**, 4516.
25. K. Yang, Y. Dai, B. Huang and Y. P. Feng, *J. Phys. D. Appl. Phys.*, 2014, **47**, 275101.
26. Q.-L. Liu, Z.-Y. Zhao and Q.-J. Liu, *RSC Adv.*, 2014, **4**, 32100.
27. Z. Zhao and Q. Liu, *Catal. Lett.*, 2008, **124**, 111.
28. Z. Zhao, Z. Li and Z. Zou, *Chemphyschem*, 2012, **13**, 3836.
29. D.-E. Gu, B.-C. Yang and Y.-D. Hu, *Catal. Commun.*, 2008, **9**, 1472.
30. Z. Zhao, Z. Li and Z. Zou, *J. Phys. Chem. C*, 2013, **117**, 6172.
31. W. Kohn, A. D. Becke and R. G. Parr, *J. Phys. Chem.*, 1996, **100**, 12974.
32. J. P. Perdew, K. Burke and M. Ernzerhof, *Phys. Rev. Lett.*, 1996, **77**, 3865.
33. J. P. Perdew, J. Chevary, S. Vosko, K. A. Jackson, M. R. Pederson, D. Singh and C. Fiolhais, *Phys. Rev. B*, 1992, **46**, 6671.
34. F. Bernardini, V. Fiorentini and D. Vanderbilt, *Phys. Rev. B*, 1997, **56**, R10024.
35. V. Anisimov, M. Korotin, J. Zaanen and O. Andersen, *Phys. Rev. Lett.*, 1992, **68**, 345.
36. X.-G. Ma, C.-Q. Tang and X.-H. Yang, *J. Theor. Comput. Chem.*, 2007, **6**, 23.
37. C. G. Van de Walle and J. Neugebauer, *J. Appl. Phys.*, 2004, **95**, 3851.
38. J. Sato, H. Kobayashi and Y. Inoue, *J. Phys. Chem. B*, 2003, **107**, 7970.
39. H. Sun, Y. Bai, Y. Cheng, W. Jin and N. Xu, *Ind. Eng. Chem. Res.*, 2006, **45**, 4971.
40. D. B. Hamal, J. A. Haggstrom, G. L. Marchin, M. A. Ikenberry, K. Hohn and K. J. Klabunde, *Langmuir.*,

2009, **26**, 2805.

41. S. Zhang, L. Song, S. Zhang, D. Sun and B. Chen, *React. Kinet. Catal. L.*, 2009, **97**, 199.

42. R. Long and N. J. English, *Chem. Phys. Lett.*, 2009, **478**, 175.

Table 1. Formation energies, average bond lengths, lattice distortions, average net charges and average dipole moments for pure, S-doped, and $Ti_{1-x}O_2S_xNM_y$ (NM = B, C, N, O, F, P, S and Cl)

Models	E_f /eV		Bond Length /Å					ΔV /Å^3	Net charge /eV				Dipole moment
	O-rich	Ti-rich	Ti-O	S-O	S-NM	Ti-NM	O-NM		Ti	O	S	NM	(Dbye)
TiO_2			1.94						1.280	-0.650			0.00 (TiO_6)
$Ti_{1-x}O_2S_x$	-16.86	10.55	1.96	1.93				-4.82	1.280	-0.68	1.54		0.663 (SO_6)
$Ti_{1-x}O_2S_xB_y$	-23.52	3.88	1.93	1.93	1.90	2.54	1.45	7.09	1.28	-0.64	1.78	0.47	0.733 (SO_6B)
$Ti_{1-x}O_2S_xC_y$	-22.59	4.81	1.99	1.94	1.80	2.50	1.25	10.77	1.28	-0.65	1.95	0.27	0.136 (SO_6C)
$Ti_{1-x}O_2S_xN_y$	-22.05	5.35	1.93	1.99	1.75	2.42	1.42	12.61	1.28	-0.65	1.36	0.09	0.791 (SO_6N)
$Ti_{1-x}O_2S_xO_y$	-21.92	5.48	1.94	2.29	1.45	2.23	2.33	10.01	1.28	-0.68	2.23	-0.8	1.049 (SO_6O)
$Ti_{1-x}O_2S_xF_y$	-18.35	9.06	1.92	2.12	2.13	1.90	2.25	12.00	1.29	-0.67	1.72	-0.46	0.701 (SO_6F)
$Ti_{1-x}O_2S_xP_y$	-21.403	6.00	1.97	2.10	2.75	2.42	1.59	17.65	1.27	-0.78	1.53	1.26	2.500 (SO_6P)
$Ti_{1-x}O_2S_xS_y$	-17.49	9.91	1.96	2.25	2.06	2.36	1.61	19.4	1.27	-0.67	1.19	0.46	3.233 (SO_6S)
$Ti_{1-x}O_2S_xCl_y$	-14.70	12.70	1.92	2.28	2.25	2.36	1.70	21.01	1.24	0.70	1.63	0.26	1.406 (SO_6Cl)

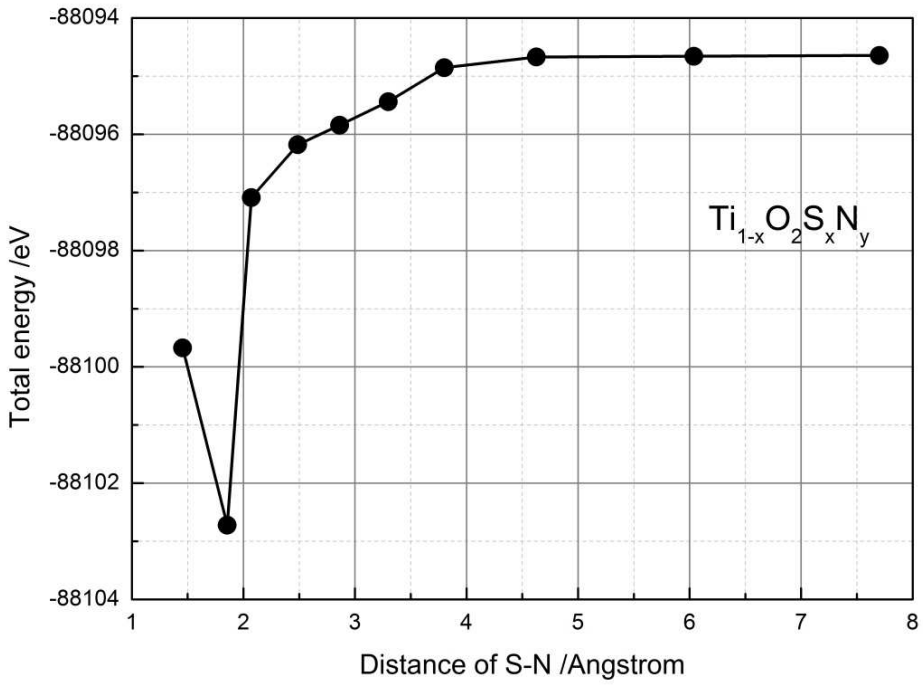

Fig 1(a). Calculated total energy as function of the distance between S and N impurities.

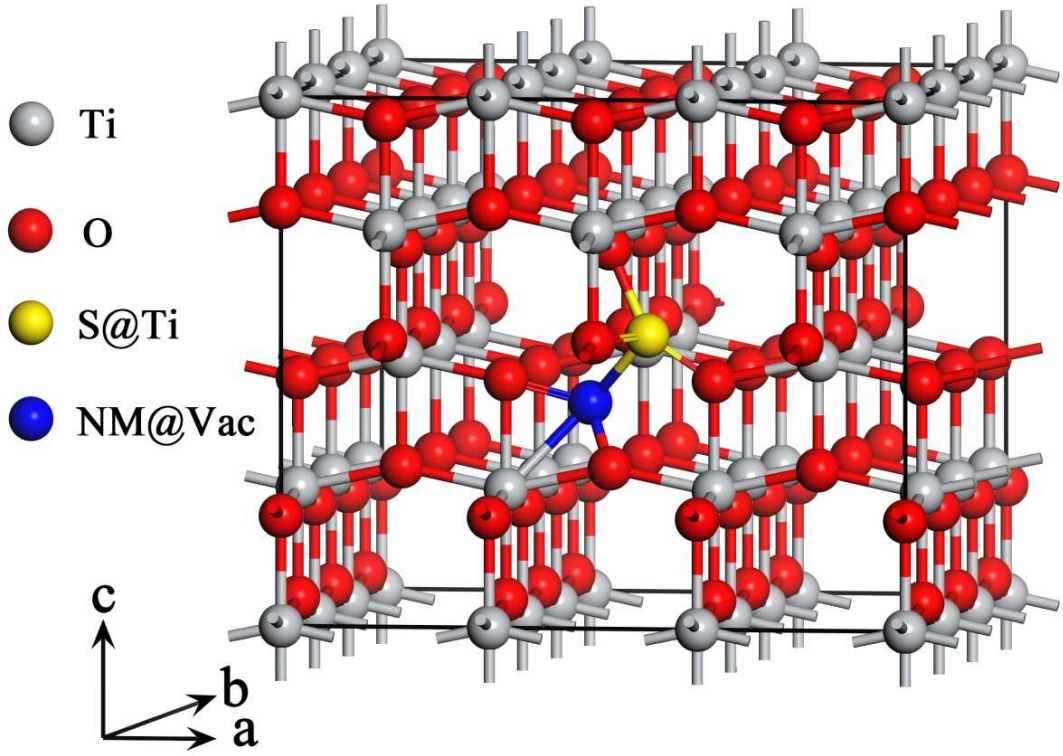

Fig. 1(b) The 3×3×1 supercell model of $Ti_{1-x}O_2S_xNM_y$ (NM = B, C, N, O, F, P, S and Cl) considered in the present work

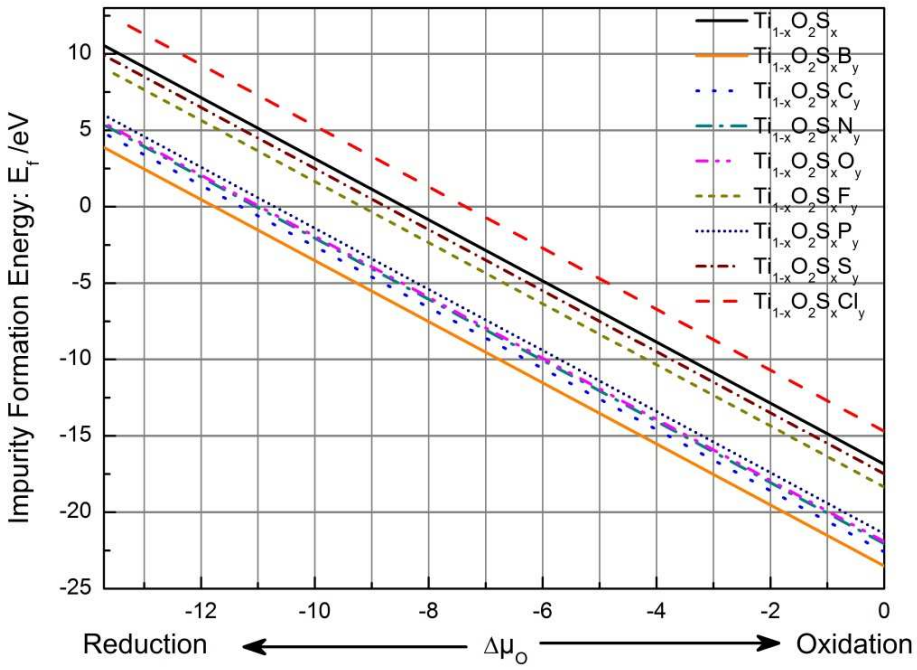

Fig. 2 Calculated impurity formation energies of different doping systems vary as a function of the difference of oxygen chemical potential

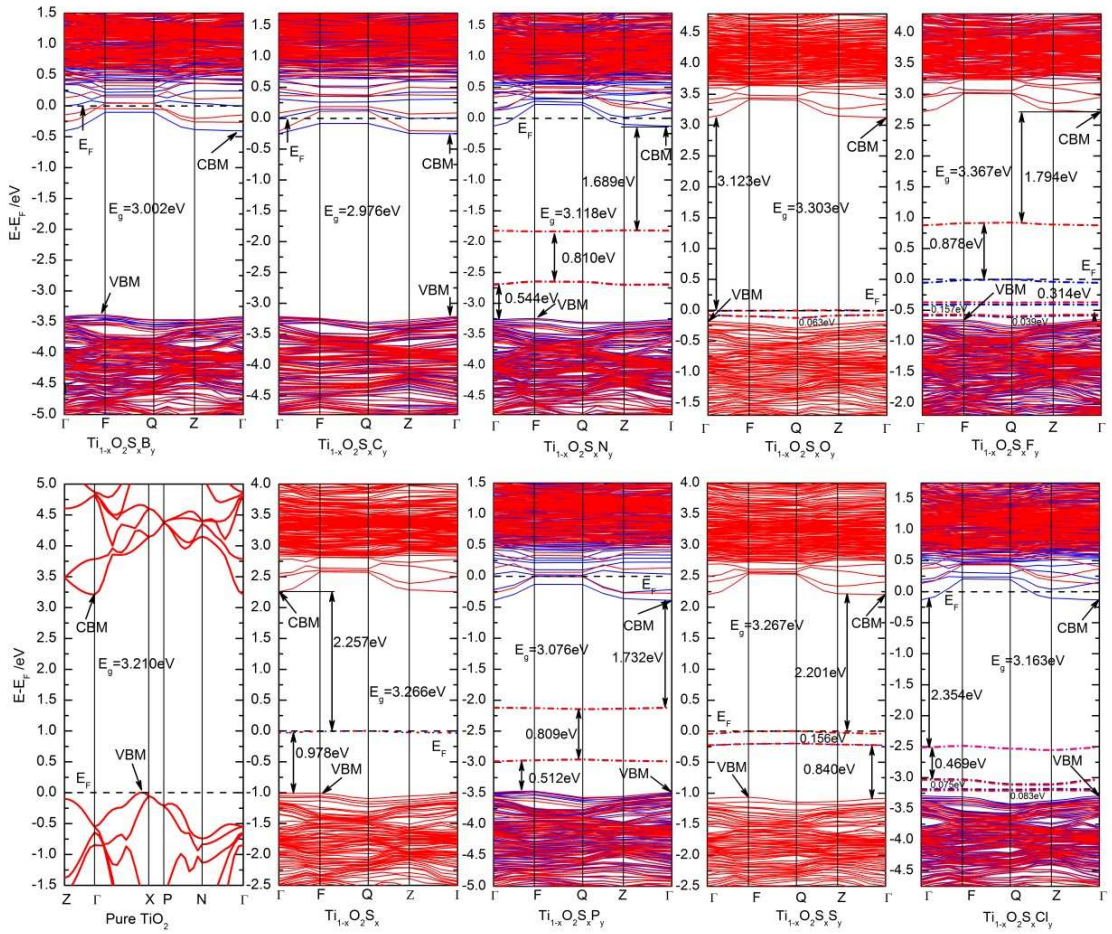

Fig.3 Calculated band structures of pure TiO_2, $Ti_{1-x}O_2S_x$, and $Ti_{1-x}O_2S_xNM_y$ (NM = B, C, N, O, F, P, S and Cl), the position of these figures are arranged by the Periodic Table

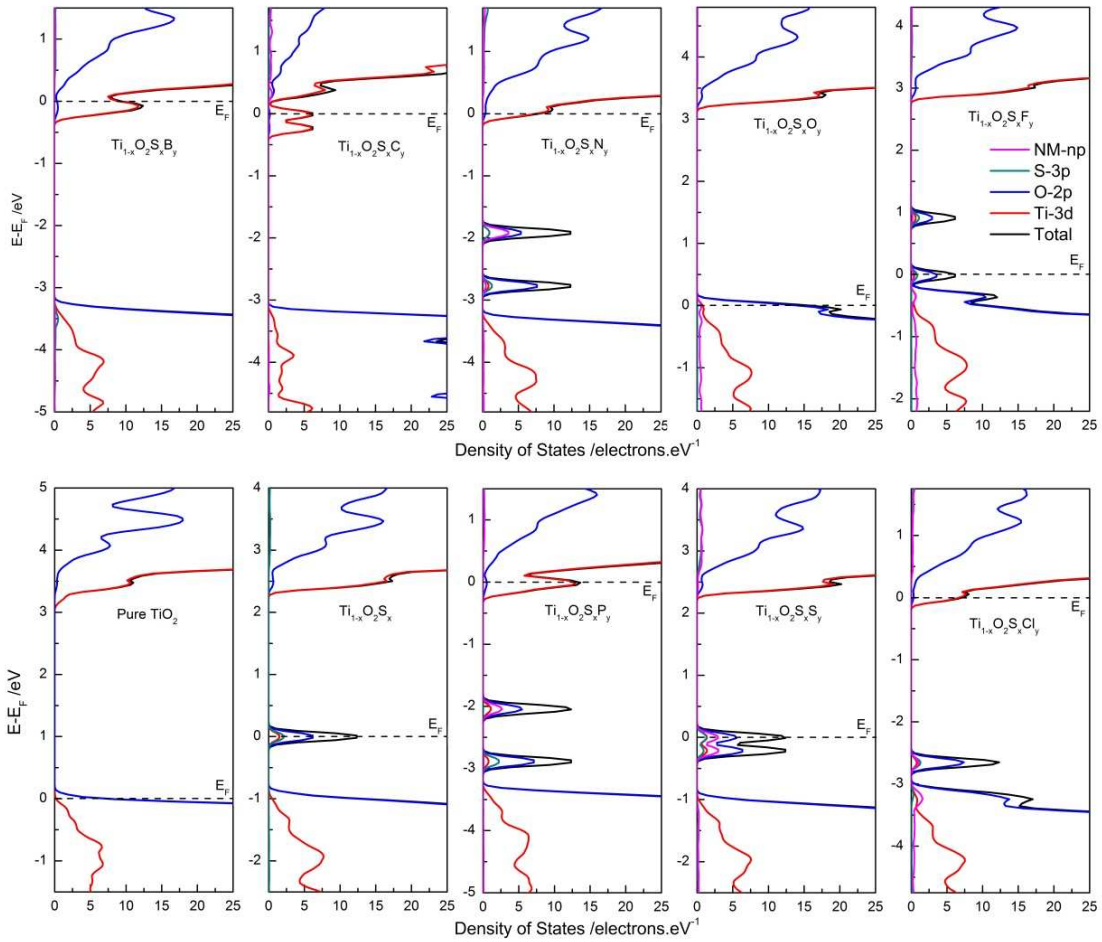

Fig. 4 Calculated total and partial density of states of pure TiO_2, $Ti_{1-x}O_2S_x$, and $Ti_{1-x}O_2S_xNM_y$ (NM = B, C, N, O, F, P, S and Cl), the position of these figures are arranged by the Periodic Table

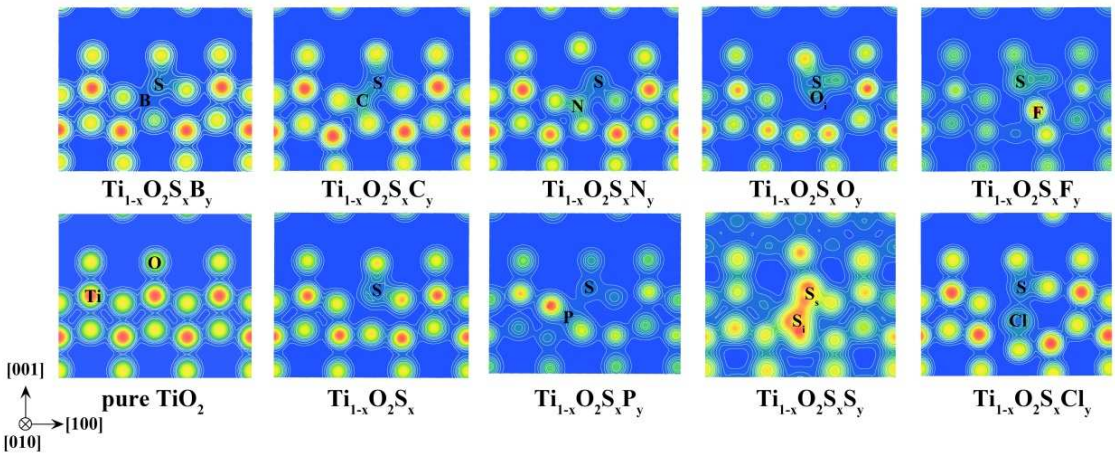

Fig. 5 Contour maps of electron density of pure TiO_2, $Ti_{1-x}O_2S_x$, and $Ti_{1-x}O_2S_xNM_y$ (NM = B, C, N, O, F, P, S and Cl), the position of these figures are arranged by the Periodic Table

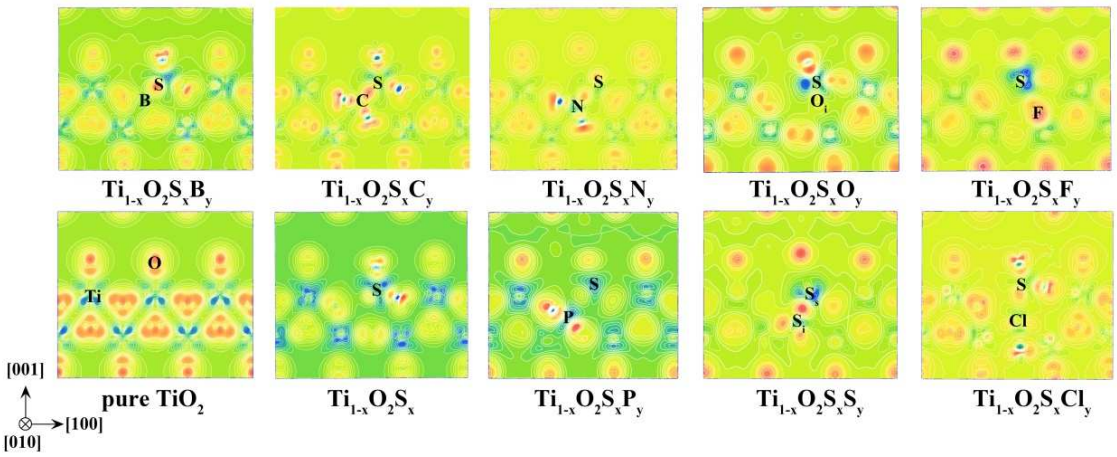

Fig. 6 Contour maps of electron density difference of pure TiO_2, $Ti_{1-x}O_2S_x$, and $Ti_{1-x}O_2S_xNM_y$ (NM = B, C, N, O, F, P, S and Cl), the position of these figures are arranged by the Periodic Table

Table of contents

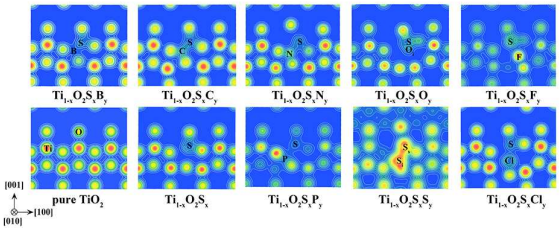

S+NM co-doping could induce the stronger local electric field and eliminate the deep impurity energy bands of S mono-doped TiO_2.